Force Spectroscopy on Dendronized Poly(*p*-phenylene)s: Revealing the Chain Elasticity and the Interfacial Interaction

Weiqing Shi, Zhiqiang Wang, Shuxun Cui, and Xi Zhang*

Key Lab of Organic Optoelectronics and Molecular Engineering, Department of Chemistry, Tsinghua University, Beijing 100084, People's Republic of China

Zhishan Bo*

State Key Laboratory of Polymer Physics and Chemistry, Institute of Chemistry, Chinese Academy of Sciences, Beijing 100080, People's Republic of China

Received July 30, 2004; Revised Manuscript Received November 10, 2004

ABSTRACT: Single-chain manipulation of two second-generation dendronized polymers, hydrophobic and amphiphilic poly(*p*-phenylene), was performed by using single-molecule force spectroscopy on the basis of atomic force microscopy. In tetrahydrofuran (THF) buffer, the individual amphiphilic dendronized polymer chain exhibits larger elasticity than the corresponding hydrophobic dendronized polymer chain does. The larger elasticity of the single amphiphilic polymer chain is probably from the collapse of oligoethyleneoxy chains in THF, which is a poor solvent for them. While using CH_2Cl_2 as a buffer, all the side groups can be expanded; the elasticity of the amphiphilic polymer chain is therefore smaller than that in THF. The individual hydrophobic polymer exhibits the same elasticity in THF and CH_2Cl_2 because of the similar polymer chain conformation in the two buffers. Moreover, the adhesion−force measurements in a poor solvent at the interface reveal that the poor solubility of the polymer side groups as well as the hydrophobic interaction between the surface and the polymer side groups enhances the adhesion force.

Introduction

A kind of novel dendrimer called dendronized polymer has attracted considerable scientific interest in recent years.[1] Dendronized polymers are dendrimers with a central linear polymeric core and attain a rodlike, cylindrical shape with the polymer backbone encapsulated into the dendritic envelope. In contrast to the conventional polymers, the diameter of the dendronized polymers is on the order of a few nanometers rather than a few angstroms.[1] The synthesis and properties of many kinds of dendronized polymers have been well documented by Schlüter and Frey in recent reviews.[1] Dendronized polymers with amphiphilic peripheral are of particular interest due to their unique structures and self-assembling properties. For example, poly(*p*-phenylene)s (PPPs) carrying Fréchet-type hydrophilic and hydrophobic dendrons at each repeat unit can form stable monolayers at air/water interface and segregate into Janus-type amphiphilic cylinders, which resemble natural ion-channel membrane proteins.[1b] AFM studies have shown that such amphiphilic cylinder can self-assemble and form giant supramolecular cylinders.[1a]

Herein, we attempt to study single-chain mechanics of dendronized PPPs using AFM-based single-molecule force spectroscopy (SMFS).With the high spatial resolution and extremely force sensitivity of AFM, the measurement of force in the piconewton (pN) range with SMFS becomes possible. From the information on the measured force−distance curves, SMFS has been widely used to investigate intramolecular and intermolecular interaction in macromolecular nanomechanics,[2] which is not accessible by conventional methods. It can provide various fingerprinting information about individual polymer chains, such as the force−extension relationship of random coils,[3] the chair-to-boat conformational transition of individual glucopyronose rings,[4] the single-molecule photomechanical cycle of azo-polymers,[5] splitting or unwinding of helical structures,[6] the detachment of single polymer chains from the substrate,[3f,7] and the polydispersity index.[8] In addition, combining SMFS with specially designed systems, researchers have directly measured host−guest interactions,[9] hydrophobic interaction,[10] and even the strength of single covalent bond,[11] and so on. Our present research focuses on revealing the elasticity of dendronized PPPs bearing hydrophobic/hydrophobic or hydrophobic/hydrophilic dendrons, as shown in Chart 1. Although AFM has been used to investigate the aggregation behavior and even to image the single chain of the dendronized polymers, there is no report on their single chain elasticity of these new nanomaterials. In addition, the dendronized polymers with diameter on the order of a few nanometers may enhance their interaction with substrate, and therefore we are wondering whether the change of the dendronized structure and the solvents can affect the conformation and adsorption energy of the dendronized PPPs on different substrates.

Experimental Section

The synthesis of dendronized polymers was reported elsewhere.[1b] For convenience, the hydrophobic dendronized poly(*p*-phenylene)s is abbreviated as hPPP, and the amphiphilic dendronized poly(*p*-phenylene)s is abbreviated as aPPP. The weight-average molecular weight (M_w) of hPPP determined by GPC with polystyrene as standards is 188 000 g/mol, and M_w/M_n is 3.0; M_w of aPPP is 85 000 g/mol, and M_w/M_n is 2.3. These numbers should be treated with carefulness because the GPC method is known to underestimate the actual molecular weight of dendronized polymers.[12] The polymers were dissolved in chloroform, and the concentration was approximately 2 mg/L.

Two kinds of slide, hydrophilic and hydrophobic, are used as adsorption substrates for the polymers. The hydrophilic

* Corresponding author. E-mail: xi@mail.tsinghua.edu.cn.

10.1021/ma048424r CCC: $30.25
Published on Web 01/11/2005

Chart 1. Chemical Structures of the Two Dendronized Polymers[a]

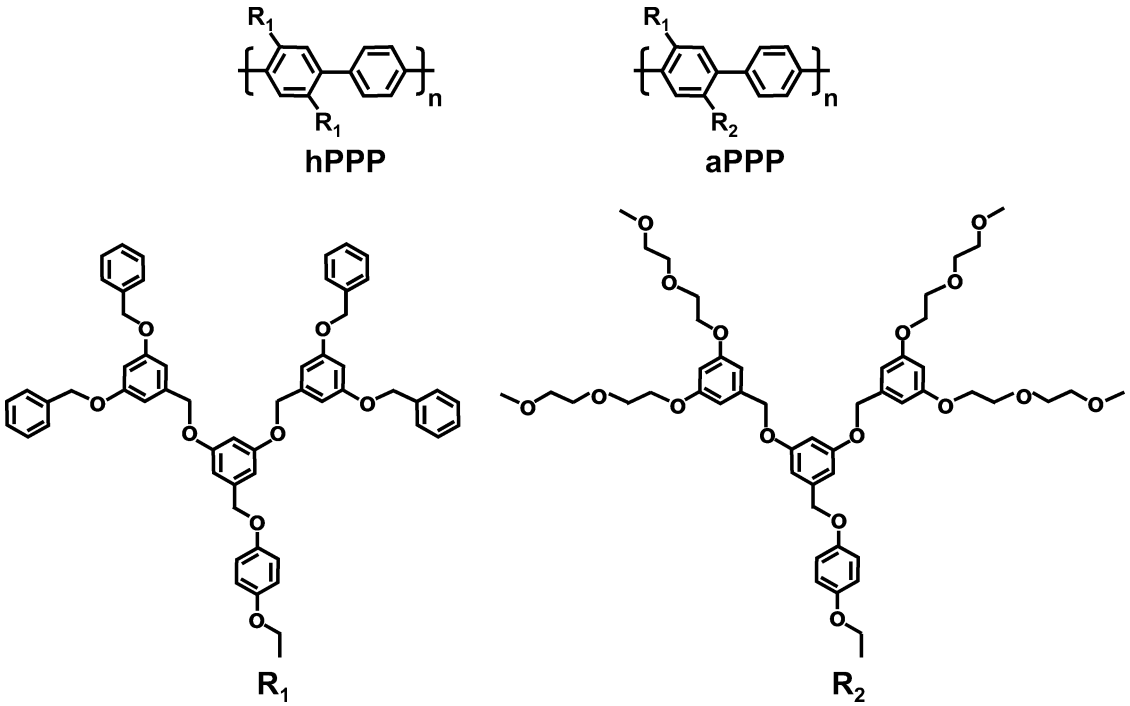

[a] The hydrophobic dendronized poly(*p*-phenylene), abbreviated hPPP, and the amphiphilic dendronized poly(*p*-phenylene), abbreviated aPPP. The side group R_1 is the hydrophobic part, and the side group R_2 is the hydrophilic part.

substrate was obtained as follows: a quartz slide was treated with a hot piranha solution (concentrated H_2SO_4/98%, H_2O_2/30%, 7/3, v/v) for 30 min, then rinsed thoroughly with deionized water (DI water), and finally dried in an oven. The surface of the cleaned slide is hydrophilic because it is covered with fresh hydroxy groups. The quartz slides were immersed into a toluene solution of dimethylmethoxypropylsilane/toluene (1:1000, v/v) for 24 h. The surface of the modified quartz slides changes to hydrophobic because the dimethylpropylsilyl groups are covered on the surface.[13] About 0.15 mL of each polymer solution was dropped on a cleaned or modified quartz slide. The slide was used in the SMFS experiment after the solution volatilized spontaneously.

The force−extension curves (in brief, force curves) have been measured at room temperature by a home-built SMFS apparatus. AFM cantilevers used in experiments were commercially available V-shaped Si_3N_4 cantilevers (Park, Sunnyvale, CA), with a spring constant ranging 0.010−0.050 N/m. Force curve measurements were made more than 500 times at different positions of the substrate for each tip/substrate combination. The stretching velocity imposed during the force measurements was about 700 nm/s, if not specified. The details of SMFS experiment have been described elsewhere.[3b,4a,6a] In brief, the polymer is physisorbed on the substrate, then a drop of tetrahydrofuran (THF) or dichloromethane (CH_2Cl_2) or DI water was put onto the substrate, and mounted between the cantilever holder and the substrate as the buffer. When the substrate contacts with the AFM tip by the movement of the piezo, polymers will adsorb to the tip and form the so-called polymer bridge between the tip and the substrate. The polymer bridge will be elongated while separating the tip and the substrate, and the cantilever will deflect by the elastic force. The deflection−extension curves were recorded and converted to force−extension curves.[2b] The data of the adhesion forces are statistically analyzed by the function in Origin 6.0 of "statistics on column", and the standard deviation is the error we want.

Results and Discussion

Single-Chain Elasticities of hPPP and aPPP Typical force curves of hPPP in THF obtained with different tips in different SMFS experiments are shown in Figure 1. All the force curves show similar features: the force value increases monotonically with the extension and then suddenly drops to zero when reaching a rupture point. The contour length of the force curves is different, which has several random factors: the molecular weight of polymers is polydisperse, the adsorption of the tip on the substrate is stochastic, and the anchor point on the polymer chains happens by chance. To compare their elasticity with different contour length, the force curves have been normalized by their extension referring to the same force (350 pN).[2,3] The normalized force curves superimpose well, as shown in the inset of Figure 1. This result indicates that the force curves reflect the single-chain elongation of the polymers.

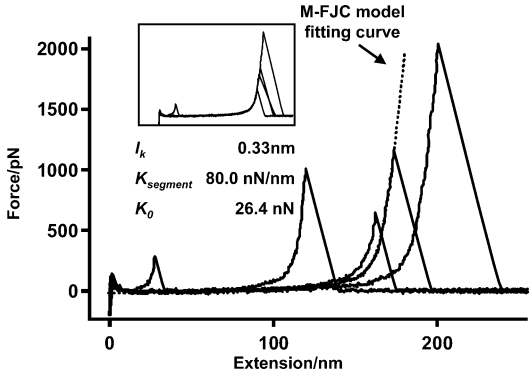

Figure 1. Several typical force−extension curves of hPPP in THF buffer. Inset: the superposition of the normalized force curves. One of the force curves is fitted by the M-FJC model curve, shown by the dashed line.

By keeping the loading force lower than the rupture force, a single polymer chain can be manipulated between the stretching and the relaxing state. There is no hysteresis between the consecutive trace/retrace pair curves of the same hPPP chain, as shown in Figure 2, which suggests that the SMFS experiment is in the

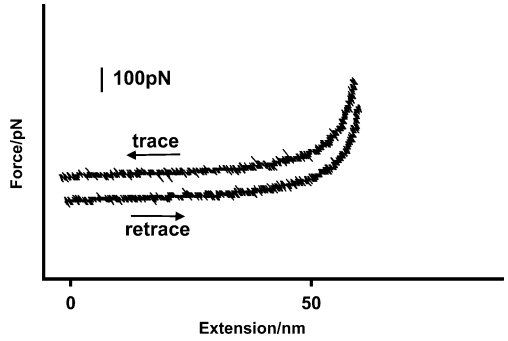

Figure 2. Successive manipulation of an hPPP single chain. The trace and the retrace force curves have no hysteresis, suggesting that the elongation in the experiment is reversible.

thermodynamic equilibrium and the stretching of a single polymer chain is reversible.

A freely jointed chain (FJC) model, which is a classical model for polymer single chain based on Langevin function, treats a polymer chain as an aggregate of many independent rigid Kuhn segments with length of l_k (Kuhn length).[14] The segments are freely jointed; i.e., there is no restriction to their spatial distribution so that each segment can point in every direction with equal probability.[2b] The elasticity of a FJC polymer chain is mainly resulted by the entropic contribution. Therefore, the FJC model cannot describe a polymer chain, which is not so flexible. To optimize the FJC model, Smith et al. introduced another parameter, the segment elasticity, and produced a modified FJC (M-FJC) model,[14] which is based on the extended Langevin function shown below. Under M-FJC model, each segment can be deformed under stress:

$$x(F) = \{\coth[(Fl_k)/(k_BT)] - (k_BT)/(Fl_k)\}(L_{contour} + nF/K_{segment})$$

Here, x represents the extension of a polymer chain (end-to-end distance), F is the applied force upon an individual polymer chain, $L_{contour}$ is the contour length of the polymer chain, Kuhn length (l_k) is the length of the statistically independent segment, n is the number of segments being stretched, which equals to $L_{contour}/l_k$, k_B is the Boltzmann constant, and T is the temperature in kelvin. The deformability of segments is characterized by the segment elasticity, $K_{segment}$. The product of the segment elasticity multiplied by the Kuhn length, K_0, represents the normalized segment elasticity of an individual polymer chain. The elasticity of a single polymer chain is contributed by both entropy and enthalpy. In the low-force regime, the elasticity is mainly governed by entropy, which reflects the contribution of the conformation change of a polymer chain, the so-called entropic elasticity. However, in the high-force regime, the elasticity is mainly controlled by enthalpy, which originates from the torsion and the rotation of the segments, the so-called enthalpic elasticity.

An M-FJC fitting curve of one typical force curve of hPPP is shown in Figure 1. All the force curves of hPPP obtained in the SMFS experiment are fitted well by M-FJC model, and the set of fitting parameters is $l_k = 0.33 \pm 0.01$ nm and $K_{segment} = 80.0 \pm 1.0$ nN/nm, though the contour lengths are different. To multiply l_k by $K_{segment}$ makes $K_0 = 26.4 \pm 1.0$ nN. The narrow distribution of the parameters indicates that the force signals are from single polymer chain elongation.

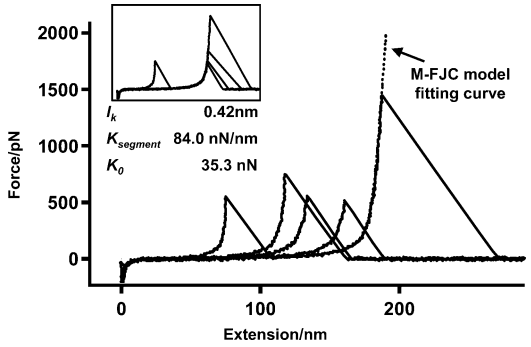

Figure 3. Several typical force−extension curves of aPPP in THF buffer. Inset: the superposition of the normalized force curves. One of the force curves is fitted by the M-FJC model curve, shown by the dashed line.

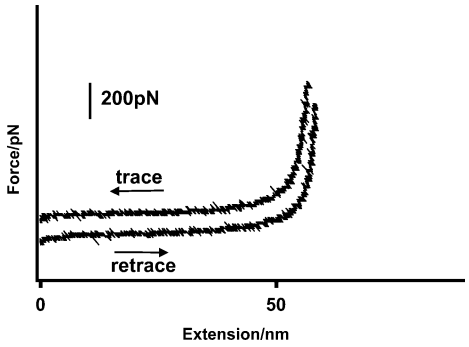

Figure 4. Successive manipulation of an aPPP single chain. The trace and the retrace force curves have no hysteresis, suggesting that the elongation in the experiment is reversible.

Similarly, we have performed single chain experiment on amphiphilic dendronized polymers. Figure 3 shows the typical force curves of aPPP with various contour lengths obtained with different tips in THF in many SMFS experiments, and the normalized force curves are superimposed well, as shown in the inset of Figure 3. The fitting curve of the M-FJC model for a typical aPPP force curve is also shown in Figure 3. The narrowly distributed parameters of all the force curves are $l_k = 0.42 \pm 0.01$ nm, $K_{segment} = 84.0 \pm 1.0$ nN/nm, and $K_0 = 35.3 \pm 1.0$ nN. The continuous stretching and relaxing manipulation of aPPP polymer chain have been performed. No hysteresis between the trace and retrace force curves is observed, as shown in Figure 4. The reversible stretching indicates a thermodynamic equilibrium condition in the experiment. According to the above proofs, the force curves can reveal the single-chain elongation of aPPP in THF.

To compare the difference of the elasticity of the two polymers in THF, their normalized force curves are shown in Figure 5. The two curves are almost superimposed in the low-force regime but branched when the force further increases. These results imply that the entropic elasticity of the two polymers is almost the same in THF, but the enthalpic elasticity of aPPP is larger than that of hPPP. The difference of the enthalpic elasticity between aPPP and hPPP may be due to their different steric effect. It is well-known that THF is not a good solvent for the oligoethyleneoxy,[15] so the peripheral oligoethyleneoxy chains of the amphiphilic dendronized polymers will collapse toward the backbone in THF solution and make the torsion and elongation of the polymer chain more difficult. As a result, the enthalpic elasticity of aPPP is larger than that of hPPP whose peripheral groups are phenyl instead of oligo-

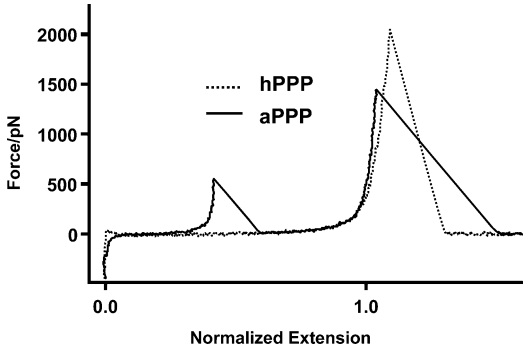

Figure 5. Comparison of the normalized force curves of hPPP and aPPP.

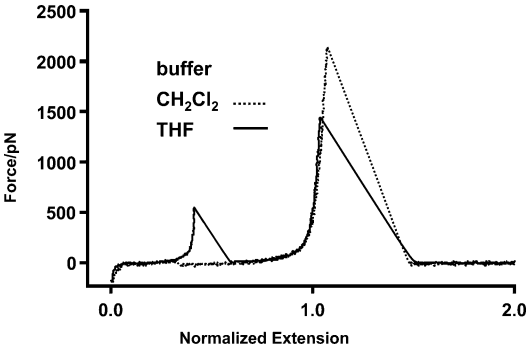

Figure 6. Comparison of the normalized force curves of aPPP in different buffer, THF vs CH_2Cl_2.

ethyleneoxy. If the steric effect of oligoethyleneoxy really exists, we would expect it decreases to some extent in a good solvent. For example, CH_2Cl_2 is a good solvent for both hydrophobic and hydrophilic side groups; oligoethyleneoxy chains should exist as a more extended conformation in CH_2Cl_2 than in THF and thus decrease the steric effect to some extent.[15] Comparing the normalized force curves of aPPP in THF and in CH_2Cl_2, we found interestingly that the enthalpic elasticity does become less strong in CH_2Cl_2 than in THF, as shown in Figure 6. The fitting parameters of the M-FJC for aPPP in CH_2Cl_2 are $l_k = 0.40 \pm 0.01$ nm, $K_{segment} = 80.0 \pm 1.0$ nN/nm, and $K_0 = 32.4 \pm 1.0$ nN. For hPPP, we did not find any elastic difference when either CH_2Cl_2 or THF used as a buffer. These facts provide further evidence that the difference of enthalpic elasticity originates from the collapse of oligoethyleneoxy chains of aPPP in THF.

Interfacial Conformation and Adhesive Energy. In addition to studying the elasticity of individual polymer chains as shown above, we are also wondering whether the SMFS can be used to probe the conformation and adhesion force of the dendronized polymers on a solid substrate.[3f,7] So we did SMFS experiments on hPPP at the interface between the hydrophobic slide and DI water, which is the poor solvent for the polymer. A typical force curve with a long plateau was obtained as shown in Figure 7A. The sharp peak in the initial part of the force curve corresponds to the very strong nonspecific adhesion between the bare tip and the uncovered regions of the substrate. The AFM tip has a curvature of 20−50 nm at its apex. Compared with the cross section of an extended polymer chain, the tip is much larger. In the case that one polymer chain is captured by the tip, only little of the apex surface area is affected and the strong interaction between the tip and substrate is retained, inducing the sharp peak in

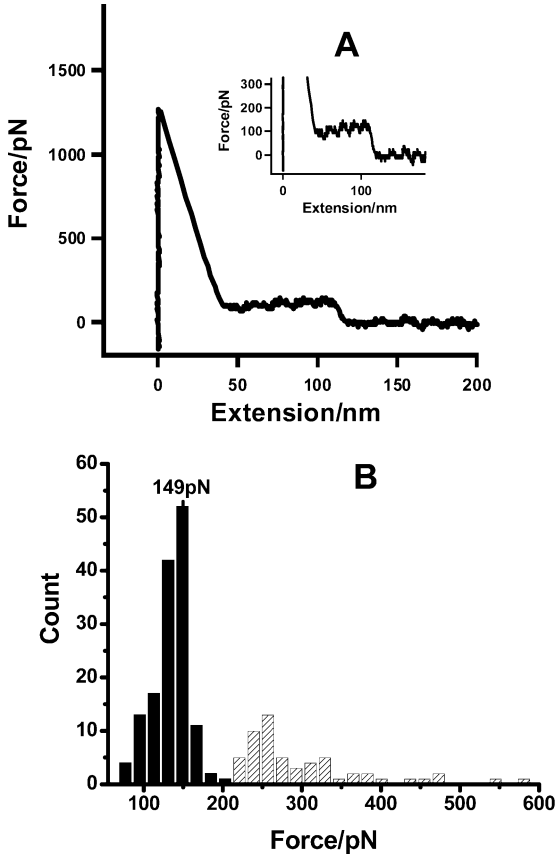

Figure 7. (A) Typical force curves of hPPP obtained on the hydrophobic substrate in DI water as buffer. The inset is the magnified plateau. (B) The histogram of height statistics of the plateau in all the force curves.

the beginning of the force curve. The following plateau of the force curve suggests that there is a constant force to desorb the polymer chain from the surface. Since there is little possibility for the polymer chains to dissolve into water, so the polymer chains have to adsorb onto the substrate with multiple adsorptive points. The external energy (the force) used to separate each adsorptive point is similar. As a consequence, the detected force curves exhibit a plateau feature. In other words, according to the plateau force curves, we can deduce that hPPP exists as a trainlike conformation on the substrate. The plateau length directly reflects the length of an detached polymer chain from the substrate, while the height of a plateau corresponds to the desorption force that is required to desorb polymers from the hydrophobic surface.[7g] According to the statistic analysis of the plateau heights, the desorption force of hPPP from the hydrophobic surface is 149 ± 20 pN, as shown in Figure 7B. Even when changing the stretching velocity from 3000 to 70 nm/s, the height of the plateau is almost the same. Thus, we can conclude that the adsorption and the desorption of the polymer chains are on a much shorter time scale than the experimental stretching process occurs,[7g] suggesting that the experiment is performed in the equilibrium state. In this case, the adhesion force is equal to the force of desorption.

The SMFS experiment of hPPP on the hydrophilic surface has shown similar results as on the hydrophobic surface: the force curves with plateaus (not shown in the figures) indicates that the conformation of the polymer chain is trainlike, whereas the height of the plateau is corresponding to the force of the polymer

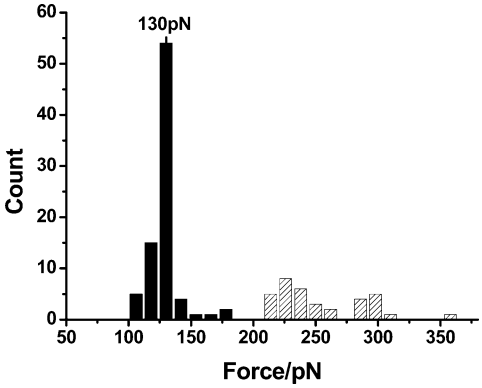

Figure 8. Desorption force of hPPP on the hydrophilic substrate in DI water as buffer.

desorbed from the hydrophilic surface. As shown in Figure 8, the desorption force is 130 ± 12 pN. Since the desorption is not stretching velocity dependent, the adhesion energy is just equal to the desorption energy. Under similar conditions, the adhesion force between hPPP and the hydrophobic surface is larger than that between hPPP and the hydrophilic surface. This result should be reasonable if we consider the contribution of the hydrophobic interaction between the surface and the adsorbed polymer chain. In the case of both adsorbate and substrate are hydrophobic, there is still a hydrophobic effect in the sites between water and substrate after the desorption of the polymer chain from the substrate. Whereas for a hydrophilic substrate, the hydrophobic effect does not exist between water and substrate after the desorption of the polymer chain from the substrate. The water molecules will occupy the surface and form hydrogen bonds with the hydroxyl groups on the substrate, which will compensate the energy at the interface in some extent. As a result, the potential barrier to desorb the polymer chain from the hydrophilic surface is lowered, as observed in the lower force in the plateau.

Similarly, we have investigated the interfacial behavior of aPPP polymer chains between hydrophobic surface and DI water. A typical force curve of aPPP on hydrophobic surface is shown in Figure 9A. The plateau indicated the conformation of aPPP polymer chains is also trainlike at the quartz (hydrophobic)/water interface. The histogram in Figure 9B is the statistic analysis of the desorption force obtained in the experiments, and the highest peak is 120 ± 15 pN. The single chain adhesion force is just the same because of the thermodynamic equilibrium during the experiment. Compared with the adhesion force of hPPP on the same type of surface, the force of aPPP is less than that of hPPP. This difference should be related to the different conformation between hPPP and aPPP. The oligoethyleneoxy chains at the periphery of aPPP can be soluble in DI water. That is to say, aPPP polymer chain should have an extended conformation toward the buffer side at the interface. But a hPPP single chain does not have the same extended trend because of its thorough hydrophobic side groups. So the contact areas of the two polymers on a hydrophobic surface are different: the area of hPPP polymer chain is more than that of aPPP polymer chain. Hence, the adhesion force of the hPPP polymer chain is larger than that of the aPPP polymer chain on the hydrophobic surface. The adhesion force of aPPP at the quartz (hydrophilic)/water interface has been obtained by the same method. According to the statistic histogram in Figure 10, the adhesion force of aPPP on the hydrophilic surface decreased to 102 ± 10 pN. The weak hydrophobic interaction between aPPP polymer chain and the hydrophilic surface induces the adhesive energy decreasing, and the peripheral oligoethyleneoxy chains still have the extended conformation toward water. These two factors are probably the reasons for the low adhesion force of aPPP on the hydrophilic surface.

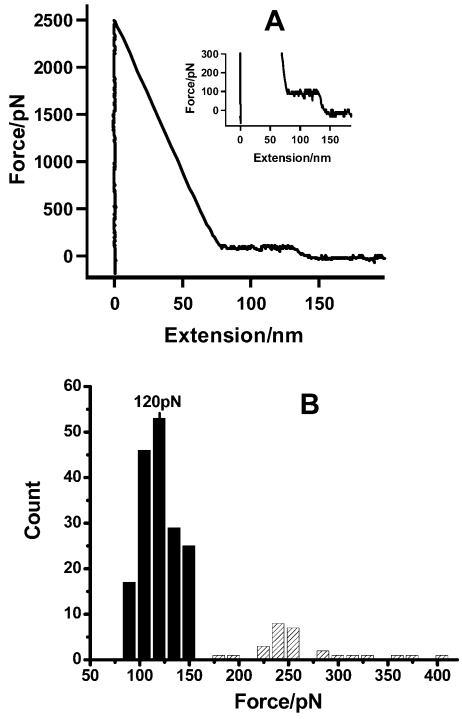

Figure 9. (A) Typical force curves of aPPP obtained on the hydrophobic substrate in DI water as buffer. The inset is the magnified plateau. (B) Histogram of height statistics of the plateau in all the force curves.

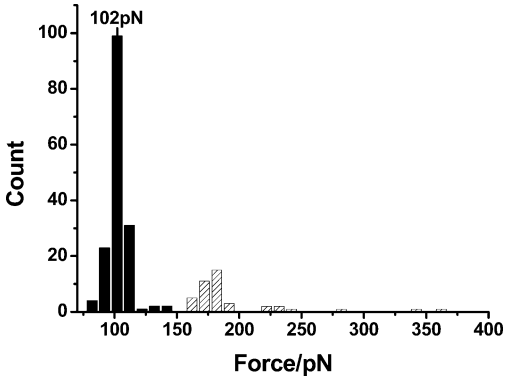

Figure 10. Desorption force of aPPP on the hydrophilic substrate in DI water as buffer.

Conclusions

Dendronized polymers with different side groups have been investigated by single-molecule force spectroscopy, and the information on their single-chain elasticity and the adhesion forces on different substrates are obtained. The amphiphilic polymer has larger single-chain elasticity than the hydrophobic polymer in THF buffer. Oligoethyleneoxy chains cannot exist in an extended conformation in THF,[15] so the hydrophilic part of amphiphilic polymer collapses to the backbone, which makes the torsion and elongation of aPPP polymer chain more difficult than that of hPPP chain. CH_2Cl_2 is a good

solvent for all the side groups of the two polymers.[15] The conformation of the polymer side groups is more extended in CH_2Cl_2 buffer than in THF buffer, so the elasticity of aPPP polymer chain is not so strong in CH_2Cl_2 as in THF. But the elasticity of hPPP is the same in CH_2Cl_2 and THF because of the same conformation of the polymer chain in the two buffers. When the substrate changes from hydrophobic to hydrophilic, in DI water buffer the adhesion force of the two polymers declines because of the weaker hydrophobic interaction strength between the hydrophilic substrate and the adsorbed polymer chains. In addition, because of the different solubility of the two polymers, the more soluble the side groups of the two polymers, the less the adhesion force.

Acknowledgment. This study was supported by the Major State Basic Research Development Program (G2000078102, 2002CB613401), the Ministry of Science and Technology, and Natural Science Foundation of China (20474035, 50073009, 20225415). We thank Prof. Hermann E. Gaub for his help in establishing the SMFS setup and Prof. A. Dieter Schlüter for kindly providing the interesting dendronized polymers.

References and Notes

(1) (a) Schlüter, A. D.; Rabe, J. P. *Angew. Chem., Int. Ed.* **2000**, *39*, 864. (b) Bo, Z. S.; Rabe, J. P.; Schlüter, A. D. *Angew. Chem., Int. Ed.* **1999**, *38*, 2370. (c) Bo, Z. S.; Schlüter, A. D. *Macromol. Rapid Commun.* **1999**, *20*, 21. (d) Frey, H. *Angew. Chem., Int. Ed.* **1998**, *37*, 2193. (e) Zhang, A. F.; Shu, L. J.; Bo, Z. S.; Schlüter, A. D. *Macromol. Chem. Phys.* **2003**, *204*, 328.

(2) (a) Zhang, W. K.; Zhang, X. *Prog. Polym. Sci.* **2003**, *28*, 1271. (b) Hugel, T.; Seitz, M. *Macromol. Rapid Commun.* **2001**, *22*, 989.

(3) (a) Yamamoto, S.; Tsujii, Y.; Fukuda, T. *Macromolecules* **2000**, *33*, 5995. (b) Li, H. B.; Liu, B. B.; Zhang, X.; Gao, C. X.; Shen, J. C.; Zou, G. T. *Langmuir* **1999**, *15*, 2120. (c) Bemis, J. E.; Akhremitchev, B. B.; Walker, G. C. *Langmuir* **1999**, *15*, 2799. (d) Zhang, W. K.; Zou, S.; Wang, C.; Zhang, X. *J. Phys. Chem. B* **2000**, *104*, 10258. (e) Wang, C.; Shi, W. Q.; Zhang, W. K.; Zhang, X.; Katsumoto, Y.; Ozaki, Y. *Nano Lett.* **2002**, *2*, 1169. (f) Hugel, T.; Grosholz, M.; Clausen-Schaumann, H.; Pfau, A.; Gaub, H. E.; Seitz, M. *Macromolecules* **2001**, *34*, 1039. (g) Shi, W. Q.; Cui, S. X.; Wang, C.; Wang, L. Y.; Zhang, X.; Wang, X. J.; Wang, L. *Macromolecules* **2004**, *37*, 1839. (h) Zou, S.; Ma, Y. J.; Hempenius, M. A.; Schönherr, H.; Vancso, G. J. *Langmuir* **2004**, *20*, 6278.

(4) (a) Rief, M.; Oesterhelt, F.; Heymann, B.; Gaub, H. E. *Science* **1997**, *275*, 1295. (b) Marszalek, P. E.; Li, H. B.; Oberhauser, A. F.; Fernandez, J. M. *Proc. Natl. Acad. Sci. U.S.A.* **2002**, *99*, 4278. (c) Marszalek, P. E.; Oberhauser, A. F.; Pang, Y. P.; Fernandez, J. M. *Nature (London)* **1998**, *396*, 661. (d) Li, H. B.; Rief, M.; Oesterhelt, F.; Gaub, H. E.; Zhang, X.; Shen, J. C. *Chem. Phys. Lett.* **1999**, *305*, 197. (e) Marszalek, P. E.; Pang, Y. P.; Li, H. B.; Yazal, J. E.; Oberhauser, A. F.; Fernandez, J. M. *Proc. Natl. Acad. Sci. U.S.A.* **1999**, *96*, 7894. (f) Xu, Q. B.; Zhang, W. K.; Zhang, X. *Macromolecules* **2002**, *35*, 871. (g) O'Donoghue, P.; Luthey-Schulten, Z. A. *J. Phys. Chem. B* **2000**, *104*, 10398. (h) Lu, Z. Y.; Nowak, W.; Lee, G.; Marszalek, P. E.; Yang, W. T. *J. Am. Chem. Soc.* **2004**, *126*, 9033.

(5) (a) Hugel, T.; Holland, B. N.; Cattani, A.; Moroder, L.; Seitz, M.; Gaub, H. E. *Science* **2002**, *296*, 1103. (b) Holland, N. B.; Hugel, T.; Neuert, G.; Cattani-Scholz, A.; Renner, C.; Oesterhelt, D.; Moroder, L.; Seitz, M.; Gaub, H. E. *Macromolecules* **2003**, *36*, 2015.

(6) (a) Li, H. B.; Rief, M.; Oesterhelt, F.; Gaub, H. E. *Adv. Mater.* **1998**, *10*, 316. (b) Rief, M.; Clausen-Schaumann, H.; Gaub, H. E. *Nat. Struct. Biol.* **1999**, *6*, 346. (c) Li, H. B.; Zhang, W. K.; Xu, W. Q.; Zhang, X. *Macromolecules* **2000**, *33*, 465. (d) Xu, Q. B.; Zou, S.; Zhang, W. K.; Zhang, X. *Macromol. Rapid Commun.* **2001**, *22*, 1163. (e) Zhang, L.; Wang, C.; Cui, S. X.; Wang, Z. Q.; Zhang, X. *Nano Lett.* **2003**, *3*, 1119.

(7) (a) Zhang, W. K.; Cui, S. X.; Fu, Y.; Zhang, X. *J. Phys. Chem. B* **2002**, *106*, 12705. (b) Seitz, M.; Friedsam, C.; Jöstl, W.; Hugel, T.; Gaub, H. E. *CHEMPHYSCHEM* **2003**, *4*, 986. (c) Haupt, B. J.; Ennis, J.; Sevick, E. M. *Langmuir* **1999**, *15*, 3886. (d) Haupt, B. J.; Senden, T. J.; Sevick, E. M. *Langmuir* **2002**, *18*, 2174. (e) Cui, S. X.; Liu, C. J.; Zhang, X. *Nano Lett.* **2003**, *3*, 245. (f) Friedsam, C.; Becares, A. D. C.; Jonas, U.; Gaub, H. E.; Seitz, M. *CHEMPHYSCHEM* **2004**, *5*, 388. (g) Friedsam, C.; Becares, A. D. C.; Jonas, U.; Seitz, M.; Gaub, H. E. *New J. Phys.* **2004**, *6*, 1.

(8) Al-Maawali, S.; Bemis, J. E.; Akhremitchev, B. B.; Leecharoen, R.; Janesko, B. G.; Walker, G. C. *J. Phys. Chem. B* **2001**, *105*, 3965.

(9) (a) Schönherr, H.; Beulen, M. J.; Bügler, J.; Huskerns, J.; Van Veggel, F. C. J. M.; Reinhoudt, D. N.; Vancso, F. J. *J. Am. Chem. Soc.* **2000**, *122*, 4963. (b) Zou, S.; Zhang, Z. H.; Förch, R.; Knoll, W.; Schönherr, H.; Vancso, G. J. *Langmuir* **2003**, *19*, 8618.

(10) Cui, S. X.; Liu, C. J.; Zhang, W. K.; Zhang, X.; Wu, C. *Macromolecules* **2003**, *36*, 3779.

(11) Grandbois, M.; Beyer, M.; Rief, M.; Clausen-Schaumann, H.; Gaub, H. E. *Science* **1999**, *283*, 1727.

(12) (a) Percec, V.; Ahn, C. H.; Barboiu, B. *J. Am. Chem. Soc.* **1997**, *119*, 12978. (b) Förster, S.; Neubert, I.; Schlüter, A. D.; Linder, P. *Macromolecules* **1999**, *32*, 4043.

(13) (a) Netzer, L.; Sagiv, J. *J. Am. Chem. Soc.* **1983**, *105*, 674. (b) Maoz, R.; Sagiv, J. *Adv. Mater.* **1998**, *10*, 580.

(14) (a) Smith, S. B.; Finzi, L.; Bustamante, C. *Science* **1992**, *258*, 1122. (b) Smith, S. B.; Cui, Y. J.; Bustamante, C. *Science* **1996**, *271*, 795.

(15) Gitsov, I.; Fréchet, J. M. J. *J. Am. Chem. Soc.* **1996**, *118*, 3785.

MA048424R